Viscoelastic Response of Double Hydrophilic Block Copolymers for Drug Delivery Applications

Achilleas Pipertzis *, Angeliki Chroni, Stergios Pispas, Jan Swenson

Posted Date: 4 June 2025

doi: 10.20944/preprints202506.0309.v1

Keywords: double hydrophilic block copolymer; densely grafted architecture; rheology; viscoelastic response

 doi:10.20944/preprints202506.0309.v1

Article

Viscoelastic Response of Double Hydrophilic Block Copolymers for Drug Delivery Applications

Achilleas Pipertzis [1,*], Angeliki Chroni [2], Stergios Pispas [2] and Jan Swenson [1]

[1] Department of Physics, Chalmers University of Technology, 41296, Gothenburg, Sweden

[2] Theoretical and Physical Chemistry Institute, National Hellenic Research Foundation, 48 Vassileos Constantinou Ave., 11635 Athens

* Correspondence: achilleas.pipertzis@chalmers.se

Abstract: This study investigates the mechanical properties of double hydrophilic block copolymers (DHBCs) based on poly[oligo(ethylene glycol) methacrylate] (POEGMA) and poly(vinyl benzyl trimethylammonium chloride) (PVBTMAC) blocks, by employing small amplitude oscillatory shear (SAOS) rheological measurements. We report that the mechanical properties of DHBCs are governed by the interfacial glass transition temperature (T_g^{inter}), verifying the disordered state of these copolymers. An increase of zero-shear viscosity can be observed by increasing the VBTMAC content, yielding a transition from liquid-like to gel-like and finally to an elastic-like response for the PVBTMAC homopolymer. By changing the block arrangement along the backbone, from statistical to sequential, a distinct change in the viscoelastic response is obvious, indicating the presence/absence of bulk-like regions. In the second part, the rheological data are analyzed within the framework of the classical free volume theories of glass formation. Specifically, the copolymers exhibit reduced fractional free volume and similar fragility values compared to the PVBTMAC homopolymer. Contrary, the activation energy increases by increasing the VBTMAC content, reflecting the required higher energy for the relaxation of the glassy VBTMAC segments. Overall, this study provides useful information about the viscoelastic properties of DHBCs with densely grafted macromolecular architecture that are promising for drug delivery applications.

Keywords: double hydrophilic block copolymer; densely grafted architecture; rheology; viscoelastic response

1. Introduction

Bottlebrush polymers, characterized by densely grafted macromolecular architecture, have attracted considerable attention owing to their highly tunable physical and chemical properties, which depend on side chain length, backbone length, and grafting density [1–8]. In comb polymers, side chains act as a solvent, diluting backbone concentration - a phenomenon known as dynamic tube dilution [4,9–11]. This effect results in low viscosity and a reduced rubbery plateau. These properties make bottlebrush block copolymers promising for applications in drug delivery, energy storage, nanostructures, catalysis, and 3D printing [12–23].

Double hydrophilic block copolymers (DHBCs), composed of two chemically distinct water-soluble blocks, are important in polymer science, pharmacy, biophysics and biochemistry [24–27]. They offer an alternative option to traditional amphiphilic block copolymers and self-assemble in aqueous conditions in response to changes in ionic strength, temperature, pH, or complexation with specific (bio)molecules. DHBCs with charged blocks, known as polyelectrolytes, are promising candidates for biomacromolecule delivery via electrostatic complexation [28]. For enhancing water solubility and stability in aqueous media, a neutral block, such as poly(ethylene glycol) or poly(oligo(ethylene glycol) methacrylate) (POEGMA), is used.

Diblock and statistical copolymers consisting of poly[oligo(ethylene glycol) methacrylate] (POEGMA) and poly(vinyl benzyl trimethylammonium chloride) (PVBTMAC) have been

 doi:10.20944/preprints202506.0309.v1

successfully synthesized using a reversible addition–fragmentation chain transfer (RAFT) polymerization process [26,27]. Recent research studies have focused on these copolymers' abilities to form electrostatic complexes with hydrophilic magnetic nanoparticles, short DNA and negatively charged proteins (i.e. insulin) [26,27]. Additionally, the relaxation dynamics and the self-assembly of these DHBCs were investigated under dry conditions [29]. It was evidenced that the weak segregation strength between the two hydrophilic blocks results in homogeneous dynamics that are governed by the interfacial glass transition temperature (T_g^{inter}) [29]. A detailed study of the viscoelastic response of these DHBCs is missing from the existing literature and such information is of interest for scientists working on these promising DHBCs for biomedical applications. It is worth noting that DHBCs with densely grafted macromolecular architecture are also promising for the design of novel solid polymer electrolytes for battery applications [19,20,22,23].

Herein, block and random DHBCs were studied by means of rheological measurements. We report that the PVBTMAC homopolymer exhibits an elastic-response up to high temperatures, reflecting its strong (i.e. rigid) nature. In the first part, the effect of the VBTMAC block on the zero-shear viscosity, determined by using two empirical models, is presented. In the second part, the rheological data are discussed with respect to classical free volume theories of glass formation. The values of fractional free volume, thermal expansion coefficient, fragility, and apparent activation energy at the glass transition temperature (T_g) are reported and compared with those of the PVBTMAC parent homopolymer.

2. Materials and Methods

2.1. Synthesis

The synthetic procedure and molecular characterization of the studied DHBCs is highlighted in previous studies [26,27]. Specifically, the charged DHBCs with densely grafted macromolecular architecture were prepared by RAFT polymerization, an advantageous method for controlling the molar mass (M_w) and achieving polydispersity values close to unity [30,31]. The chemical structure of the investigated DHBCs is depicted in Figure 1.

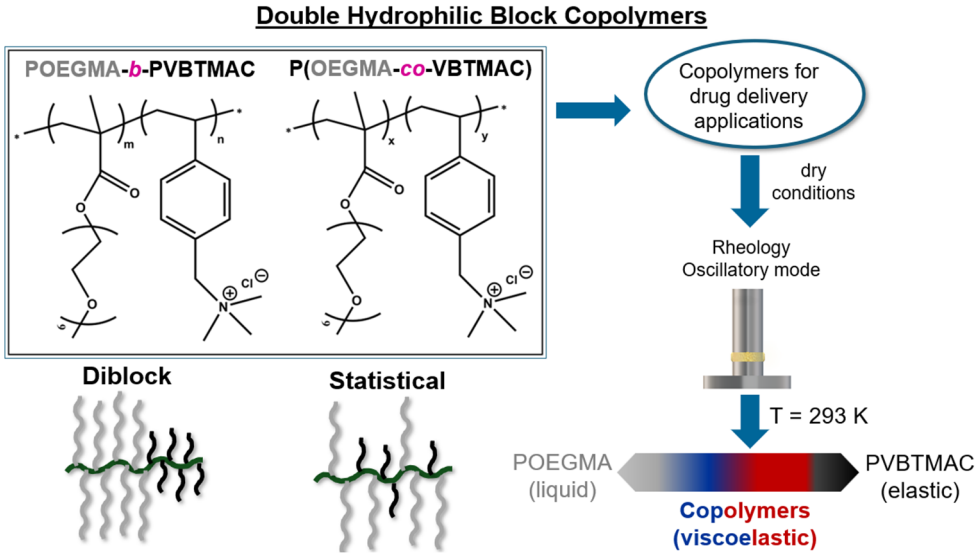

Figure 1. Chemical structure of the dried block and random DHBCs along with a schematic of the block sequence along the backbone and a description of the motivation of this study.

2.2. Rheology

Rheological measurements into the linear viscoelastic regime (LVR) can provide quantitative insight into the viscoelastic response of the studied polymeric materials [32]. A MCR-302 twin mode

 doi:10.20944/preprints202506.0309.v1

rheometer by Anton Paar was used for the identification of the viscoelastic properties of grafted copolymers under dry conditions. Measurements were made with the environmental test chamber as a function of temperature, by using the heating system (P-PTD200). The samples were prepared on the lower rheometer plate with a diameter of 8 mm. Specifically, the upper plate was brought into contact, and the sample thickness was adjusted accordingly. Typically, the gap between plates ranged between 0.3 mm to 0.6 mm, among the investigated DHBCs. At each temperature the linear viscoelastic region of the copolymers was determined by performing strain sweeps of the complex shear moduli $|G^*|$ from 0.01 to 50% (the upper limit varies regarding the state of the material), at ω = 10 rad·s^{-1}, as shown in **Figure S1**. Subsequently, isothermal frequency sweeps in an angular frequency range of $0.1 < \omega < 100$ rad·s^{-1} were carried out in temperature steps of 10 K, by employing the extracted strain amplitude of the dynamic strain sweep. Before each isothermal measurement, a thermal stabilization of 20 min was employed to ensure thermal equilibrium. Data collected under the minimum torque of the instrument were excluded. Master curves were constructed by using the principle of time-temperature superposition (tTs). For estimating the zero-shear viscosity, we used an extrapolation procedure for the data that do not reach the Newtonian limit at low frequencies. Empirical models can be utilized to fit the complex viscosity response and extrapolate to low frequencies to estimate the value of zero-shear viscosity, η_0. Specifically, the Carreau-Yasuda (CY) model is given by the following equation [33,34]:

$$\eta^*(\omega) = \eta_0[1 + (\lambda\omega)^{\alpha}]^{\frac{n-1}{\alpha}} \quad (1)$$

where, λ is the relaxation time, α indicates the width of the transition region between Newtonian and power-law behavior and n is the power-law index (i.e. a measure of the shear-thinning nature of a polymer melt). All these parameters can be obtained by fitting the measured data. Another empirical model that can be used for fitting the viscosity data is the modified Cross (MC) model, according to [35]:

$$\eta^*(\omega) = \frac{\eta_0}{1 + [C_0\omega]^{1-n}} \quad (2)$$

where, C_0 and n can be extracted by fitting the data to Equation 2.

3. Results and Discussion

Quantitative insight into the viscoelastic response of the dried DHBCs can be obtained through small amplitude oscillatory shear (SAOS) rheological measurements. The effect of temperature under isochronal conditions (i.e. at a fixed angular frequency of 10 rad·s^{-1}) on the mechanical properties of the dried copolymers is depicted in **Figure S2**. The PVBTMAC homopolymer exhibits elastic behavior up to extremely high temperatures, indicating its rigid/strong nature. The temperature dependence of the loss factor verifies the existence of two T_gs, associated with the backbone and side chain vitrification [29]. Regarding the statistical copolymers, at a fixed temperature, they exhibit reduced shear moduli that is attributable to the influence of the soft OEGMA segments. Additionally, the viscoelastic response is governed by T_g^{inter}, defined at the crossing point of shear storage (G') and loss (G'') moduli, verifying their disordered and well mixed state, as observed by X-ray diffraction [29].

The dynamic frequency sweeps into the linear viscoelastic response under isothermal conditions (i.e. 293 K), for the statistical copolymers with various compositions are shown in Figure 2.

 doi:10.20944/preprints202506.0309.v1

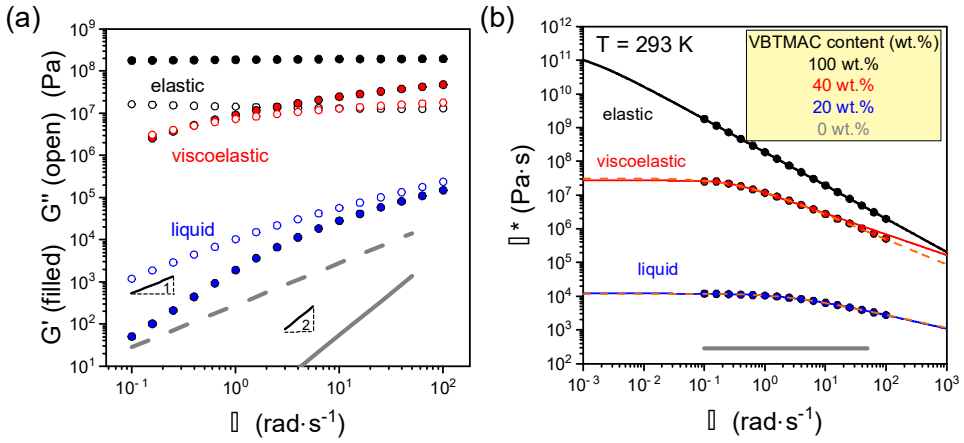

Figure 2. Angular frequency dependence of **(a)** the storage (filled symbols) and loss (open symbols) shear moduli and **(b)** complex viscosity for P(OEGMA$_{80}$-*co*-VBTMAC$_{20}$) (blue symbols) and P(OEGMA$_{60}$-*co*-VBTMAC$_{40}$) (red symbols) DHBCs and their respective homopolymers POEGMA (grey symbols) and PVBTMAC (black symbols), at a temperature of 293 K. Lines with slopes 1 and 2 are also shown in **(a)**. The solid and dashed lines in **(b)** represent fits by Eq. 1 and Eq. 2, respectively.

Initially, the dynamic frequency sweep unveils that the PVBTMAC homopolymer exhibits a strong nature and elastic response ($G' >> G'' \sim \omega^0$). In going to the statistical copolymer containing 40 wt.% VBTMAC, a viscoelastic response, characterized by comparable and frequency-dependent storage (G') and loss (G'') moduli, can be observed. By further decreasing the VBTMAC content to 20 wt.%, a liquid-like response ($G' \sim \omega^2$ and $G'' \sim \omega^1$) is evident. In the latter copolymer, the complex viscosity ($\eta^* = \sqrt{G'^2 + G''^2}/\omega$), exhibits a plateau at lower angular frequencies, from which the zero-shear viscosity, η_0 can be extracted. For extracting the zero-shear viscosity, the measured data were fitted/modelled with two different empirical models, as detailed in the experimental section. The fitting parameters are provided in Table 1. In addition, the dynamic frequency data of the statistical copolymers are compared and contrasted with those found at PVBTMAC homopolymer under iso-T_g temperatures (i.e. T_g + 30 K), in **Figure S3**. The iso-T_g comparison reflects the changes in viscoelastic response from elastic to viscoelastic and liquid response by decreasing the VBTMAC content, quantitatively verifying the observations at ambient temperature.

Table 1. Zero-shear viscosity and fitting parameters of CY and MC models.

VBTMAC (wt.%)	η_0 (Pa·s)	λ (s)	n	a
Carreau-Yasuda (CY) model				
20 (sequential)	(3 ± 1) × 10^7	580 ± 10	0.11 ± 0.02	2 (fixed)
20 (statistical)	11970 ± 30	0.43 ± 0.01	0.59 ± 0.01	0.91 ± 0.03
40 (statistical)	(2.68± 0.08) × 10^7	3.8 ± 0.3	0.38 ± 0.02	2.0 ± 0.4
100	(2 ± 2) × 10^{11}	2000 ± 1000	0.015 ± 0.002	0.99 ± 0.2
Modified Cross (MC) model				
20 (sequential)	(3 ± 1) × 10^7	1800 ± 900	0.11 ± 0.02	-
20 (statistical)	11970 ± 30	0.43 ± 0.01	0.61 ± 0.01	-
40 (statistical)	(3.13 ± 0.08) × 10^7	2.65 ± 0.4	0.25 ± 0.04	-
100	(2.47 ± 0.09) × 10^{11}	1490 ± 60	0.015 ± 0.002	-

Concerning the statistical copolymers, the relaxation time, λ, increases by increasing the concentration of VBTMAC glassy blocks. The extracted values of the power law index, n imply a shear-thinning behavior of the copolymer melts, that becomes stronger by increasing VBTMAC content. For the copolymer with 40 wt.% VBTMAC and the PVBTMAC homopolymer, the values of

 doi:10.20944/preprints202506.0309.v1

zero-shear viscosity extracted from MC model are slightly higher than the one obtained from CY model.

The effect of block arrangement along the backbone can be discussed with respect to Figure 3 and Table 1, comparing the dynamic frequency sweep data of the sequential and statistical copolymer with a VBTMAC content of 20 wt.%.

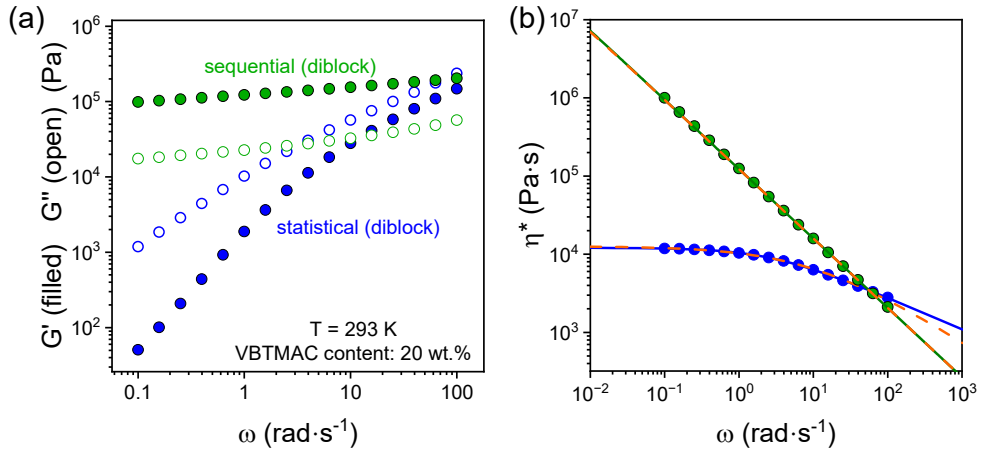

Figure 3. Angular frequency dependence of **(a)** the storage (filled symbols) and loss (open symbols) shear moduli and **(b)** complex viscosity for the sequential (green) and statistical (blue) DHBCs with 20 wt.% of VBTMAC. The solid and dashed lines in **(b)** represent fits by Eq. 1 and Eq. 2, respectively.

The sequential arrangement of VBTMAC glassy blocks yields an elastic-response ($G' >> G''$ and G', $G' \sim \omega^0$), compared to the liquid-like response of the statistical copolymer, indicating the presence of larger and continuous bulk-like VBTMAC regions, despite the fact that both specimens are into the disordered state, as evidenced in our previous study [29]. Parenthetically, a reduced change of heat capacity for T_g^{inter} was evidenced for the sequential copolymer compared to the statistical, verifying the aforementioned observations [29]. The determination of the zero-shear viscosity is challenging and inaccurate for the sequential copolymer, due to its predominantly elastic response, even at elevated temperatures (see **Figures S4** and **S5)**, hindering the low-frequency plateau in the viscosity data. To mitigate this challenge, the viscosity data were fitted with the empirical models of Eq.1 and 2, yielding a higher value of zero shear viscosity by approximately 3 orders of magnitude, compared to the corresponding statistical copolymer. This indicates that the block arrangement along the copolymer backbone plays a crucial role in tailoring the viscoelastic response of the studied DHBCs.

The extracted values for zero-shear viscosity are summarized in Figure 4.

 doi:10.20944/preprints202506.0309.v1

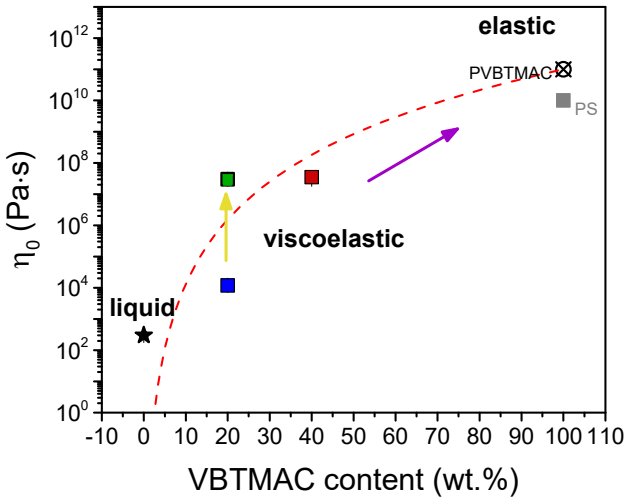

Figure 4. A Zero-shear viscosity, η_0, as a function of the VBTMAC weight fraction in DHBCs and the corresponding parent homopolymers, at ambient temperature. The zero-shear viscosity for Polystyrene (PS) is also included for comparison and taken from Ref [36]. The yellow and purple arrows indicate the effect of block arrangement across the backbone and the impact of VBTMAC content on the zero-shear viscosity, respectively. The red dashed line is guide for the eye.

The dynamic frequency sweeps for the statistical copolymers are presented at different temperatures in **Figure S6**, along with the temperature dependence of the extracted power law index. The latter increases by increasing temperature, implying less shear thinning behavior, as evident from the flattening of the viscosity curves.

Detailed information about the viscoelastic response of the studied copolymers can be obtained through the construction of master curves by employing the *tT*s principle, which involved the horizontal shifting of dynamic frequency sweeps, as shown in Figure 5.

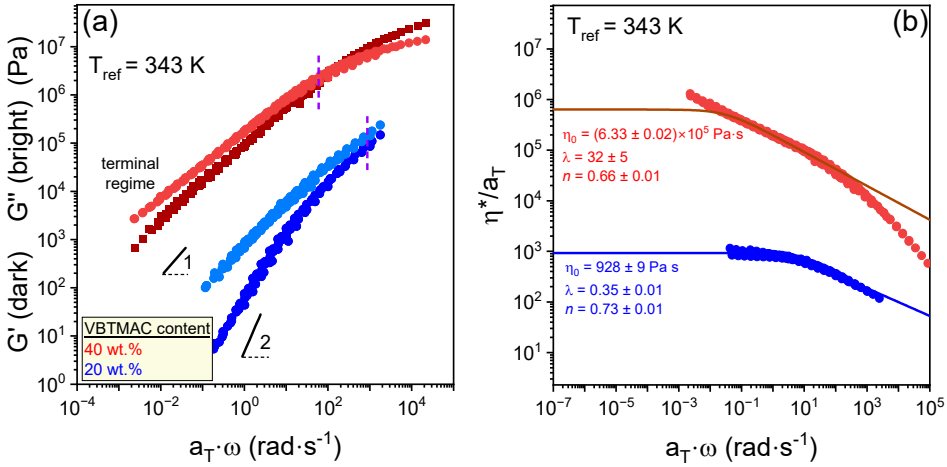

Figure 5. Superimposed master curves of **(a)** the storage (dark symbols) and loss (bright symbols) shear moduli and **(b)** complex viscosity constructed by employing the principle of *tT*s, for the statistical DHBCs with 20 wt.% (blue symbols) and 40 wt.% (red symbols) VBTMAC content, as indicated. Lines with slopes 1 and 2 are also shown in **(a)**. The solid lines represent fits by Eq. 2 in **(b)**.

For the copolymer containing 20 wt.% VBTMAC, a well-defined terminal regime ($G' \sim \omega^2$ and $G'' \sim \omega$) is observed, confirming its liquid- or melt-like behavior. In contrast, the copolymer with 40 wt.%

 doi:10.20944/preprints202506.0309.v1

VBTMAC maintains a viscoelastic response even at high temperatures (i.e., low frequencies), highlighting the influence of the glassy VBTMAC segments. As depicted in Figure 5 and **Figure S2**, the absence of large rubbery plateaus is attributable to the low molar masses and the short side chain lengths, that distinctly reduce the entanglements. Figure 5(b) presents the normalized complex viscosity, adjusted using horizontal shift factors, as a function of normalized angular frequency. This representation of the master curves for the statistical copolymers confirms the viscosity variation with copolymer composition. Simultaneously, the extracted values of power law index, by employing the MC model, indicates that both statistical copolymers display comparable levels of shear thinning behavior. The temperature dependence of the extracted horizontal shift factors is depicted in Figure 6.

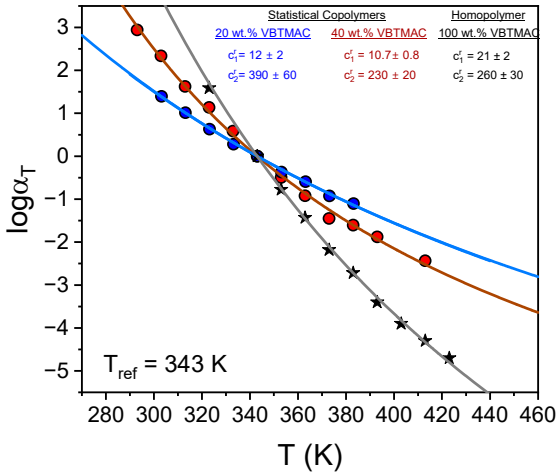

Figure 6. Temperature dependence of the horizontal shift factors for the studied DHBCs and the PVBTMAC homopolymer.

The results can now be discussed in terms of classical free volume theories of glass formation [32]. As shown in Figure 6, the extracted shift factors, α_T, were fitted according to the WLF equation [37]:

$$\log \alpha_T = -\frac{c_1^r (T - T^r)}{c_2^r (T - T^r)} \quad (3)$$

where, c_1^r and c_2^r are empirical parameters at the reference temperature, that is T_r = 343 K, for the studied DHBCs and PVBTMAC homopolymer. According to the theory, the empirical parameters can be calculated at T_g; $c_1^g = c_1^r c_2^r/(c_2^r + T_g - T_r)$ and $c_2^g = c_2^r + T_g - T_r$, and then the fractional free volume, f(T_g), and the thermal expansion coefficient of free volume, α_f, can be extracted, according to:

$$f(T_g) = \frac{1}{2.303 c_1^g} \quad (4)$$

$$\alpha_f = \frac{f(T_g)}{c_2^g} \quad (5)$$

Furthermore, the fragility or steepness index, m^*, and apparent activation energy, E_g can be estimated from [38,39]:

$$m^* = \frac{c_1^g T_g}{c_2^g} \quad (6)$$

$$E_g = 2.303R \frac{c_1^g}{c_2^g} T_g^2 \quad (7)$$

The estimated parameters are summarized in Table 2 and can be discussed with respect to Figure 7 and Figure 8.

 doi:10.20944/preprints202506.0309.v1

Table 2. Rheological T_g and WLF parameters, fractional free volume, thermal expansion coefficient, fragility along with apparent activation energy at T_g for DHBCs and PVBTMAC homopolymer.

Sample code	T_g (K)*	c_1^g	c_2^g (K)	f(T_g)	α_f (K^{-1})	m*	E_g (kJ·mol^{-1})
P(OEGMA$_{80}$-*co*-VBTMAC$_{20}$)	290	13.33	360	0.0326	9.05 × 10^{-5}	28	65.1
P(OEGMA$_{60}$-*co*-VBTMAC$_{40}$)	310	12.49	197	0.0347	1.51 × 10^{-4}	23	99.9
PVBTMAC	383	17.9	303	0.024	9.1 × 10^{-5}	23	166

* The T_g determined from rheology is higher compared to the dielectric one, due to the fact that the dynamic frequency sweeps performed at ω = 10 rad·s^{-1}.

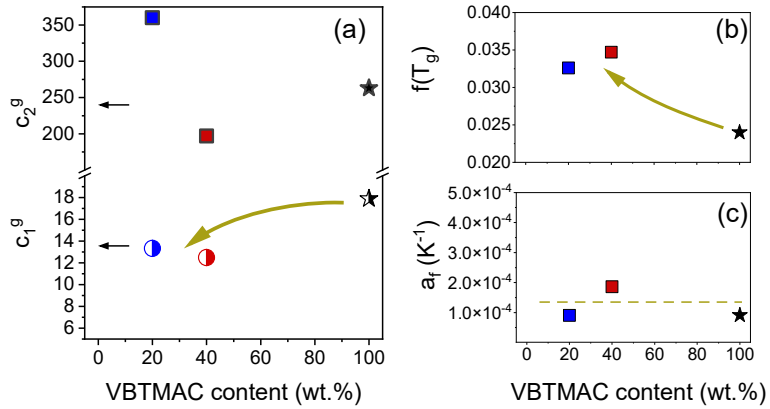

Figure 7. (a) WLF coefficients; c_1^g (semi-filled symbols) and c_2^g (filled symbols), **(b)** fractional free volume, and **(c)** thermal expansion coefficient of free volume at T_g, determined through rheology, plotted as a function of the VBTMAC content.

The copolymers exhibit slightly increased fractional free volume in relation to the PVBTMAC homopolymer, indicating the effect of the soft OEGMA segments, that further increase the free volume between the segments. These differences in fractional free volumes are primarily correlated to changes in T_g values between the PVBTMAC homopolymer and the statistical copolymers, that are mirrored to the c_1^g parameter. Instead, the c_2^g parameter appears to have a peculiar dependence on the VBTMAC content and distinctly decreases by increasing the VBTMAC content from 20 wt.% to 40 wt.%, yielding slight changes to the thermal expansion coefficient of DHBCs. The latter is in proximity to the one found for the PVBTMAC homopolymer. Importantly, the c_2^g of PVBTMAC is four times larger compared to Polystyrene (PS) [40], thereby reducing fragility values, as discussed below with respect to Figure 8a.

The effect of the VBTMAC composition on the fragility and apparent activation energy are discussed in relation to Figure 8.

 doi:10.20944/preprints202506.0309.v1

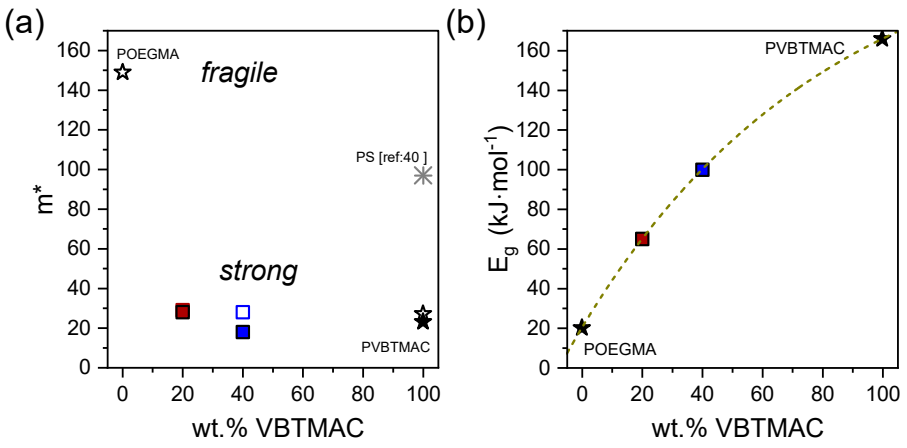

Figure 8. (a) Fragility and **(b)** apparent activation energy as a function of the VBTMAC weight fraction for the copolymers (squares) and their parent blocks (stars). Fragility data from dielectric measurements, taken from ref [29] are also included along with fragility data for PS taken from ref [40].

Noteworthy, the PVBTMAC homopolymer exhibits one of the lowest fragility values, ever reported for common polymers (see **Figure S7** and **Table S1**), reflecting a *superstrong* behavior [41,42]. The rheology-derived values are in line with those found from dielectric measurements [29]. This low value of fragility indicates a less-cooperative character of the structural relaxation, meaning that less neighboring segments cooperate in the structural relaxation. Specifically, the PVBTMAC homopolymer exhibits distinctly reduced fragility values compared to the linear Polystyrene [40,43]. A similar trend has been observed in the family of poly(*p*-alkyl methacrylates), where a change from a "fragile" ($m = 92$) to a "strong" ($m = 36$) liquid occurs only by increasing the length of the side chain with the addition of a methylene unit (see **Figure S8**) [43,44]. Specifically, the PVBTMAC homopolymer exhibits a slightly lower value of fragility than poly(*p*-alkyl methacrylates) with side chain lengths, p, bearing $1 < p < 18$ methylene units, [44–46] and the poly(*p*-phenylene) homopolymer,[47] bearing side chain length with 8 methylene units, despite the higher T_g of PVBTMAC. Therefore, the superstrong nature of the PVBTMAC homopolymer is probably driven by mainly its side chain length and its high T_g that is mainly dictated by the strong electrostatic interactions, taking place along its side chains.

Concerning the statistical copolymers, a similar *superstrong* behavior can be observed. Anticipately, as shown in Figure 8b, the apparent activation energy strongly increases by increasing the VBTMAC content, reflecting the stiff nature of VBTMAC segments and the higher amount of energy that is required for their segmental relaxation. To sum up, by analyzing the rheological results within the framework of the classical free volume theories of T_g, quantitative insight into the physical behavior of DHBCs can be obtained.

4. Conclusions

Herein, we investigate the mechanical properties of block and random DHBCs using rheological measurements. We report that the mechanical properties are governed mainly by the interfacial T_g. Depending on the VBTMAC content and block arrangement across the backbone, the macroscopic mechanical properties change from elastic-like to liquid-like. Specifically, the PVBTMAC homopolymer exhibits an elastic-response up to high temperatures, reflecting its strong nature. A viscoelastic response is evident for the statistical copolymer with 40 wt.% VBTMAC. By further decreasing the VBTMAC to 20 wt.%, the statistical copolymer exhibits a liquid-like response. Overall, the zero-shear viscosity, determined by fitting the measured data with two empirical models (i.e. Carreau-Yasuda and Modified Cross model), exponentially increases by increasing the VBTMAC content. Furthermore, for the 20 wt.% VBTMAC content, the change of block arrangement of the

 doi:10.20944/preprints202506.0309.v1

backbone from statistical to sequential results in a transition from liquid-like to elastic-like behavior, accompanied by an increase in zero-shear viscosity.

In terms of classical free volume theories [32], we report that the copolymers exhibit reduced fragility reminiscent with that found in the PVBTMAC parent block. Importantly, the PVBTMAC homopolymer exhibits 5-fold lower fragility than the one found for Polystyrene, reflecting its *superstrong* nature. The above observations are in line with previously reported dielectric results [29]. A *superstrong* behavior is also evident for the statistical copolymers, reflecting the impact of the glassy VBTMAC segments and their miscible state. To sum up, this study provides useful viscoelastic data related to densely brush copolymer that are promising for drug delivery applications.

Supplementary Materials: The following supporting information can be downloaded at the website of this paper posted on Preprints.org, Figure S1: Strain sweep test, Figure S2: Temperature ramp of shear storage and loss modulus, along with the loss factor curves, Figure S3: Angular frequency sweeps at iso-T_g temperatures, Figure S4: temperature ramps for diblock and statistical copolymer with 20 wt.% of VBTMAC, Figure S5: Angular frequency sweeps for diblock copolymer at two temperatures, Figure S6: Complex viscosity curves and the extracted power law index at different temperatures, Figure S7-S8: Comparison of fragility values with literature reported data, Table S1: glass temperature, fragility and apparent activation energy of common polymers

Author Contributions: Conceptualization, A.P.; Methodology, A.P. and A.C.; Validation, A.P., S.P. and J.S.; Formal Analysis, A.P.; Investigation, A.P.; Resources, A.C.; Data Curation, A.P.; Writing – Original Draft Preparation, A.P.; Writing – Review & Editing, A.P., A.C., S.P., J.S.; Visualization, A.P.; Supervision, S.P., and J.S.; Funding Acquisition, J.S.

Funding: A.P. and J.S. were financially supported by the Area of Advance Materials Science at the Chalmers University of Technology.

Institutional Review Board Statement: Not applicable

Data Availability Statement: Data will be made available on request.

Conflicts of Interest: The authors declare no conflicts of interest.

Abbreviations

The following abbreviations are used in this manuscript:

DHBCs	double hydrophilic block copolymers
POEGMA	poly[oligo(ethylene glycol) methacrylate]
PVBTMAC	poly(vinyl benzyl trimethylammonium chloride)
SAOS	small amplitude oscillatory shear
T_g^{inter}	interfacial glass transition temperature
RAFT	reversible addition−fragmentation chain transfer
T_g	glass transition temperature
LVR	linear viscoelastic regime
CY	Carreau-Yasuda model
MC	modified Cross model
$\|G^*\|$	complex shear moduli
G'	shear storage moduli
G''	shear loss moduli
η_0	zero-shear viscosity
tTs	time-temperature superposition
α_T	horizontal shift factor
$f(T_g)$	fractional free volume at T_g
α_f	thermal expansion coefficient of free volume at T_g
m^*	fragility
E_g	apparent activation energy
PS	Polystyrene

 doi:10.20944/preprints202506.0309.v1

References

1. Tsukahara, Y.; Kohjiya, S.; Tsutsumi, K.; Okamoto, Y. On the intrinsic viscosity of poly (macromonomer) s. *Macromolecules* **1994**, *27* (6), 1662-1664.
2. Neugebauer, D.; Zhang, Y.; Pakula, T.; Sheiko, S. S.; Matyjaszewski, K. Densely-grafted and double-grafted PEO brushes via ATRP. A route to soft elastomers. *Macromolecules* **2003**, *36* (18), 6746-6755.
3. Vlassopoulos, D.; Fytas, G.; Loppinet, B.; Isel, F.; Lutz, P.; Benoit, H. Polymacromonomers: Structure and dynamics in nondilute solutions, melts, and mixtures. *Macromolecules* **2000**, *33* (16), 5960-5969.
4. Kapnistos, M.; Vlassopoulos, D.; Roovers, J.; Leal, L. Linear rheology of architecturally complex macromolecules: Comb polymers with linear backbones. *Macromolecules* **2005**, *38* (18), 7852-7862.
5. Hu, M.; Xia, Y.; McKenna, G. B.; Kornfield, J. A.; Grubbs, R. H. Linear rheological response of a series of densely branched brush polymers. *Macromolecules* **2011**, *44* (17), 6935-6943.
6. Daniel, W. F.; Burdyńska, J.; Vatankhah-Varnoosfaderani, M.; Matyjaszewski, K.; Paturej, J.; Rubinstein, M.; Dobrynin, A. V.; Sheiko, S. S. Solvent-free, supersoft and superelastic bottlebrush melts and networks. *Nature materials* **2016**, *15* (2), 183-189.
7. Qian, Z.; Chen, D.; McKenna, G. B. Re-visiting the "consequences of grafting density on the linear viscoelastic behavior of graft polymers". *Polymer* **2020**, *186*, 121992.
8. Jang, J.; Leo, C. M.; Santiago, P.; Kennemur, J. G. Unraveling the Linear-to-Bottlebrush Transition by Linear Viscoelastic Response to Increasing Side Chain Length. *Macromolecules* **2025**.
9. Daniels, D.; McLeish, T.; Crosby, B.; Young, R.; Fernyhough, C. Molecular rheology of comb polymer melts. 1. Linear viscoelastic response. *Macromolecules* **2001**, *34* (20), 7025-7033.
10. Lee, J. H.; Fetters, L. J.; Archer, L. A. Stress relaxation of branched polymers. *Macromolecules* **2005**, *38* (26), 10763-10771.
11. Roovers, J.; Graessley, W. Melt rheology of some model comb polystyrenes. *Macromolecules* **1981**, *14* (3), 766-773.
12. Saha, D.; Witt, C. L.; Fatima, R.; Uchiyama, T.; Pande, V.; Song, D.-P.; Fei, H.-F.; Yavitt, B. M.; Watkins, J. J. Opportunities in Bottlebrush Block Copolymers for Advanced Materials. *ACS nano* **2024**, *19* (2), 1884-1910.
13. Cui, S.; Zhang, B.; Shen, L.; Bates, F. S.; Lodge, T. P. Core–shell gyroid in ABC bottlebrush block terpolymers. *Journal of the American Chemical Society* **2022**, *144* (47), 21719-21727.
14. Song, Q.; Dong, Q.; Liang, R.; Xue, Y.; Zhong, M.; Li, W. Hierarchical self-assembly of ABC-type bottlebrush copolymers. *Macromolecules* **2023**, *56* (14), 5470-5481.
15. Detappe, A.; Nguyen, H. V.-T.; Jiang, Y.; Agius, M. P.; Wang, W.; Mathieu, C.; Su, N. K.; Kristufek, S. L.; Lundberg, D. J.; Bhagchandani, S. Molecular bottlebrush prodrugs as mono-and triplex combination therapies for multiple myeloma. *Nature nanotechnology* **2023**, *18* (2), 184-192.
16. Pan, T.; Dutta, S.; Kamble, Y.; Patel, B. B.; Wade, M. A.; Rogers, S. A.; Diao, Y.; Guironnet, D.; Sing, C. E. Materials design of highly branched bottlebrush polymers at the intersection of modeling, synthesis, processing, and characterization. *Chemistry of Materials* **2022**, *34* (5), 1990-2024.
17. Lapkriengkri, I.; Albanese, K. R.; Rhode, A.; Cunniff, A.; Pitenis, A. A.; Chabinyc, M. L.; Bates, C. M. Chemical Botany: Bottlebrush Polymers in Materials Science. *Annual Review of Materials Research* **2024**, *54* (1), 27-46.
18. Tu, S.; Choudhury, C. K.; Luzinov, I.; Kuksenok, O. Recent advances towards applications of molecular bottlebrushes and their conjugates. *Current Opinion in Solid State and Materials Science* **2019**, *23* (1), 50-61.
19. Zardalidis, G.; Pipertzis, A.; Mountrichas, G.; Pispas, S.; Mezger, M.; Floudas, G. Effect of polymer architecture on the ionic conductivity. Densely grafted poly (ethylene oxide) brushes doped with LiTf. *Macromolecules* **2016**, *49* (7), 2679-2687.
20. Pipertzis, A.; Kafetzi, M.; Giaouzi, D.; Pispas, S.; Floudas, G. A. Grafted Copolymer Electrolytes Based on the Poly (acrylic acid-co-oligo ethylene glycol acrylate)(P (AA-co-OEGA)) Ion-Conducting and Mechanically Robust Block. *ACS Applied Polymer Materials* **2022**, *4* (10), 7070-7080.
21. Rolland, J.; Brassinne, J.; Bourgeois, J.-P.; Poggi, E.; Vlad, A.; Gohy, J.-F. Chemically anchored liquid-PEO based block copolymer electrolytes for solid-state lithium-ion batteries. *Journal of Materials Chemistry A* **2014**, *2* (30), 11839-11846.

 doi:10.20944/preprints202506.0309.v1

22. Shim, J.; Bates, F. S.; Lodge, T. P. Superlattice by charged block copolymer self-assembly. *Nature communications* **2019**, *10* (1), 2108.
23. Zhang, B.; Zheng, C.; Sims, M. B.; Bates, F. S.; Lodge, T. P. Influence of charge fraction on the phase behavior of symmetric single-ion conducting diblock copolymers. *ACS Macro Letters* **2021**, *10* (8), 1035-1040.
24. Pispas, S. Double hydrophilic block copolymers of sodium (2-sulfamate-3-carboxylate) isoprene and ethylene oxide. *Journal of Polymer Science Part A: Polymer Chemistry* **2006**, *44* (1), 606-613.
25. Mountrichas, G.; Pispas, S. Novel double hydrophilic block copolymers based on poly (p-hydroxystyrene) derivatives and poly (ethylene oxide). *Journal of Polymer Science Part A: Polymer Chemistry* **2007**, *45* (24), 5790-5799.
26. Chroni, A.; Forys, A.; Sentoukas, T.; Trzebicka, B.; Pispas, S. Poly [(vinyl benzyl trimethylammonium chloride)]-based nanoparticulate copolymer structures encapsulating insulin. *European Polymer Journal* **2022**, *169*, 111158.
27. Chroni, A.; Forys, A.; Trzebicka, B.; Alemayehu, A.; Tyrpekl, V.; Pispas, S. Poly [oligo (ethylene glycol) methacrylate]-b-poly [(vinyl benzyl trimethylammonium chloride)] Based Multifunctional Hybrid Nanostructures Encapsulating Magnetic Nanoparticles and DNA. *Polymers* **2020**, *12* (6), 1283.
28. Al-Tahami, K.; Singh, J. Smart polymer based delivery systems for peptides and proteins. *Recent patents on drug delivery & formulation* **2007**, *1* (1), 65-71.
29. Pipertzis, A.; Chroni, A.; Pispas, S.; Swenson, J. Molecular Dynamics and Self-Assembly in Double Hydrophilic Block and Random Copolymers. *The Journal of Physical Chemistry B* **2024**, *128* (45), 11267-11276.
30. Moad, G.; Rizzardo, E.; Thang, S. H. Radical addition–fragmentation chemistry in polymer synthesis. *Polymer* **2008**, *49* (5), 1079-1131.
31. Skandalis, A.; Sentoukas, T.; Selianitis, D.; Balafouti, A.; Pispas, S. Using RAFT Polymerization Methodologies to Create Branched and Nanogel-Type Copolymers. *Materials* **2024**, *17* (9), 1947.
32. Ferry, J. D. *Viscoelastic properties of polymers*; John Wiley & Sons, 1980.
33. Carreau, P. J. Rheological equations from molecular network theories. *Transactions of the Society of Rheology* **1972**, *16* (1), 99-127.
34. Yasuda, K. Investigation of the analogies between viscometric and linear viscoelastic properties of polystyrene fluids. Massachusetts Institute of Technology, 1979.
35. Cross, M. M. Rheology of non-Newtonian fluids: a new flow equation for pseudoplastic systems. *Journal of colloid science* **1965**, *20* (5), 417-437.
36. Wagner, M. H.; Narimissa, E.; Poh, L.; Shahid, T. Modeling elongational viscosity and brittle fracture of polystyrene solutions. *Rheologica Acta* **2021**, *60* (8), 385-396.
37. Plazek, D. J.; Ngai, K. L. Correlation of polymer segmental chain dynamics with temperature-dependent time-scale shifts. *Macromolecules* **1991**, *24* (5), 1222-1224.
38. Qin, Q.; McKenna, G. B. Correlation between dynamic fragility and glass transition temperature for different classes of glass forming liquids. *Journal of Non-Crystalline Solids* **2006**, *352* (28-29), 2977-2985.
39. Angell, C. Spectroscopy simulation and scattering, and the medium range order problem in glass. *Journal of Non-Crystalline Solids* **1985**, *73* (1-3), 1-17.
40. Pipertzis, A.; Hossain, M. D.; Monteiro, M. J.; Floudas, G. Segmental dynamics in multicyclic polystyrenes. *Macromolecules* **2018**, *51* (4), 1488-1497.
41. Huang, D.; McKenna, G. B. New insights into the fragility dilemma in liquids. *The Journal of chemical physics* **2001**, *114* (13), 5621-5630.
42. Böhmer, R.; Ngai, K. L.; Angell, C. A.; Plazek, D. J. Nonexponential relaxations in strong and fragile glass formers. *The Journal of chemical physics* **1993**, *99* (5), 4201-4209.
43. Kunal, K.; Robertson, C. G.; Pawlus, S.; Hahn, S. F.; Sokolov, A. P. Role of chemical structure in fragility of polymers: a qualitative picture. *Macromolecules* **2008**, *41* (19), 7232-7238.
44. Floudas, G.; Štepánek, P. Structure and dynamics of poly (n-decyl methacrylate) below and above the glass transition. *Macromolecules* **1998**, *31* (20), 6951-6957.
45. Pipertzis, A.; Hess, A.; Weis, P.; Papamokos, G.; Koynov, K.; Wu, S.; Floudas, G. Multiple segmental processes in polymers with cis and trans stereoregular configurations. *ACS Macro Letters* **2018**, *7* (1), 11-15.

 doi:10.20944/preprints202506.0309.v1

46. Pipertzis, A.; Skandalis, A.; Pispas, S.; Floudas, G. Nanophase Segregation Drives Heterogeneous Dynamics in Amphiphilic PLMA-b-POEGMA Block-Copolymers with Densely Grafted Architecture. *Macromolecular Chemistry and Physics* **2024**, *225* (19), 2400180.
47. Mierzwa, M.; Floudas, G.; Neidhöfer, M.; Graf, R.; Spiess, H. W.; Meyer, W. H.; Wegner, G. Constrained dynamics in supramolecular structures of poly (p-phenylenes) with ethylene oxide side chains: A combined dielectric and nuclear magnetic resonance investigation. *The Journal of chemical physics* **2002**, *117* (13), 6289-6299.